3D microstructure modeling and simulation of materials in lithium-ion battery cells

Julian Feinauer[1], Daniel Westhoff[1], Klaus Kuchler[1], and Volker Schmidt[1]

Institute of Stochastics, Ulm University,
Helmholtzstraße 18, 89069 Ulm, Germany
julian.feinauer@uni-ulm.de

Abstract. The microstructure of lithium-ion battery electrodes has a major influence on the performance and durability of lithium-ion batteries. In this paper, an overview of a general framework for the simulation of battery electrode microstructures is presented. A multistep approach is used for the generation of such particle-based materials. First, a 'host lattice' for the coarse structure of the material and the placement of particles is generated. Then, several application-specific rules, which, e.g., influence connectivity are implemented. Finally, the particles are simulated using Gaussian random fields on the sphere. To show the broad applicability of this approach, three different applications of the general framework are discussed, which allow to model the microstructure of anodes of energy and power cells as well as of cathodes of energy cells. Finally, the validation of such models as well as applications together with electrochemical transport simulation are presented.

Keywords: Stochastic 3D microstructure modeling, Lithium-ion cell anodes, Lithium-ion cell cathodes, Gaussian random fields on the sphere

1 Introduction

The usage of lithium-ion battery cells is steadily growing in various fields of daily life. This implies the necessity for further improvement of battery materials. As laboratory experiments are expensive in time and costs, model-based simulations of electrochemical processes in battery cells have become an important part of battery research. Simulations are also necessary for the optimization of charging strategies and control systems [1].

Electrochemical simulation models go back to the famous work of Newman and co-workers [2]. However, these models neglect detailed geometry information of the cell and its 3D microstructure by using averaged characteristics. Recently, spatially resolved transport models have been developed to simulate the charge transport in lithium-ion battery cells [3, 4].

In this work, the focus is on stochastic 3D microstructure models. Such models can be used as spatial input information for spatially resolved transport models, where highly resolved image data of 3D microstructures of battery electrodes

are necessary for model calibration. The major advantage of the combination of stochastic microstructure models with spatially resolved transport models is that this approach can be used for realistic simulations of local effects. This includes lithium-plating and further aging mechanisms which are influenced by local potentials. Furthermore, the computational complexity of this approach can be minimized for specific applications like cycle-life simulations by reduced basis methods [5]. An example of a structure generated by such a 3D microstructure model is shown in Fig. 1.

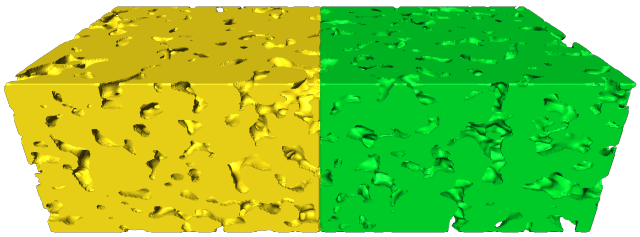

Fig. 1. Comparison of experimental and simulated anode structures. Experimental data (left), simulated data (right).

2 Simulation of lithium-ion cell electrodes

2.1 General approach

Methods of stochastic geometry and spatial statistics have been proven to be a viable tool for the simulation of 3D microstructures of energy materials like those used in fuel cells or solar cells [6–8]. The general idea of these methods is to provide microstructure models based on a few parameters that are able to generate 3D microstructures which are similar in a statistical sense to those observed in experimental data. This means that averaged characteristics like volume fractions or specific surface areas but also more refined descriptors of microstructures like tortuosity of transportation paths or the pore size distribution are in good agreement, see [9] and [10] for more details.

Furthermore, these models and the corresponding simulation algorithms are off-grid meaning that they can be used to generate structures on arbitrary length scales. The computation time it takes to generate a realization of such a microstructure model is usually very small. Thus, the usual problems of tomographic imaging related with the generation of a sufficiently large amount of

highly resolved 3D images in sufficiently large regions of interest can be solved once such a model is developed and fitted to experimental data.

2.2 Modeling framework

The microstructures of different types of lithium-ion battery electrodes vary from each other, however, they share some common structural properties. In general, electrodes consist of systems of connected particles that can have complex shapes. For the electrode models it is very important to fit fundamental microstructure characteristics like porosity and specific surface area exactly [11]. Another important characteristic of the electrodes is the high connectivity of particles. This means that each particle is connected to many neighboring particles. Thus, the model of individual particle sizes and shapes has to be flexible enough to meet all these conditions.

A general framework based on a stochastic particle model which possesses these properties has been developed. It is based on the representation of particles as linear combinations of spherical harmonics which can then be seen as realizations of Gaussian random fields (GRFs) on the sphere. Particles with random sizes and shapes can be simulated using GRFs on the sphere whose parameters are fitted to the coefficients of the spherical harmonics expansions of particles extracted from experimental data [12]. The whole framework consists of several steps, which are described in more detail in the following subsections:

- approximation of particles
- particle model
- host lattice, particle arrangement
- connectivity of particles
- particle placement and boundary conditions
- simulation of individual particles

Approximation of particles. As our aim is to develop a stochastic model for irregularly shaped particles of electrode materials, a first step is to find a suitable (analytical) representation of the particles observed in tomographic images. Thus, each particle is transformed into an analytical function by applying an expansion in spherical harmonic functions.

The spherical harmonic functions form a basis of the family of square-integrable functions defined on the unit sphere. This means that every square-integrable function can be written as an expansion in spherical harmonics. This is pretty similar to the well-known Fourier series expansion that is frequently used in signal processing.

In such an expansion the spherical harmonics have a natural ordering by their degree l and their order m. Regarding our application this means that spherical harmonic functions with higher order l represent smaller features of the particle surfaces. This motivates the truncation of the series of spherical harmonic functions at a certain cutoff degree L which leads to a good approximation of the particles.

On the one hand, this is necessary for numerical calculations and it makes further modeling easier. But, on the other hand, this is a nice possibility to smooth the particles in a 'natural' way to minimize artifacts resulting, e.g., from measurements, binarization or (particle) segmentation. Of course, a good choice of the parameter L is crucial and thus has been investigated in detail in [12].

Images showing the experimental microstructure before and after the smoothing of particles by the usage of spherical harmonics are given in Fig. 2. A more detailed comparison for an individual particle can be found in Fig. 3.

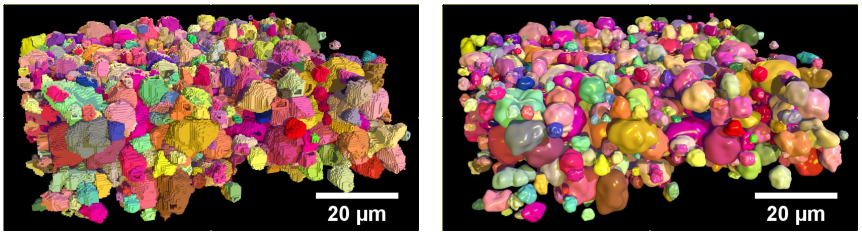

(a) (b)

Fig. 2. Comparison of the result of structural segmentation and approximation of particles by spherical harmonics. Particle system before (a), and after approximation by spherical harmonics (b). Reprinted from [12] with permission from Elsevier.

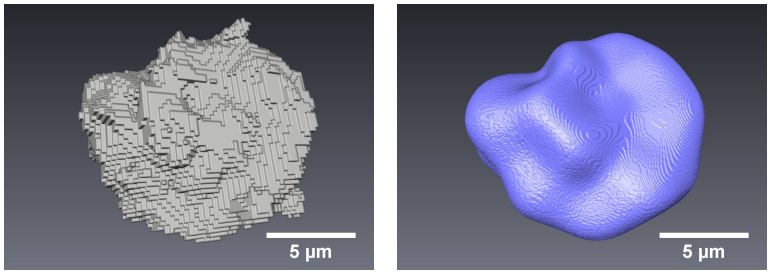

(a) (b)

Fig. 3. Example of a particle from an energy cell anode. Segmented particle from tomographic image (a) and approximation of the particle with a truncated series of spherical harmonics for $L = 10$ (b). Reprinted from [12] with permission from Elsevier.

Particle model. As described above, particles in electrode materials are often 'sphere-like' but no perfect spheres, see Fig. 3(a). Thus, simple approaches where particle models are based on spheres, like, e.g., in [13] are not sufficiently precise, especially since the volume fraction as well as the surface area of particles plays

an important role for the functionality of the material, see, e.g., [14, 15]. Thus, an alternative method which allows great flexibility, namely Gaussian random fields on the sphere, lead to a better accuracy of the model.

Gaussian random fields on the sphere are a model to describe the surface of randomly shaped objects. The idea is to generate a random radius function (in spherical coordinates) that assigns a radius value to each point (or angle) on the sphere. Of course, these values are not totally independent but have a spatial correlation. The exact spatial correlation can be controlled by the so-called angular power spectrum (APS) which is related to the Fourier spectrum in the 1D analogy. Thus, for a given material the APS has to be calculated for particles from experimental data and can then be used to generate random particles. An example of the APS for random particles from an energy cell is shown in Fig. 4.

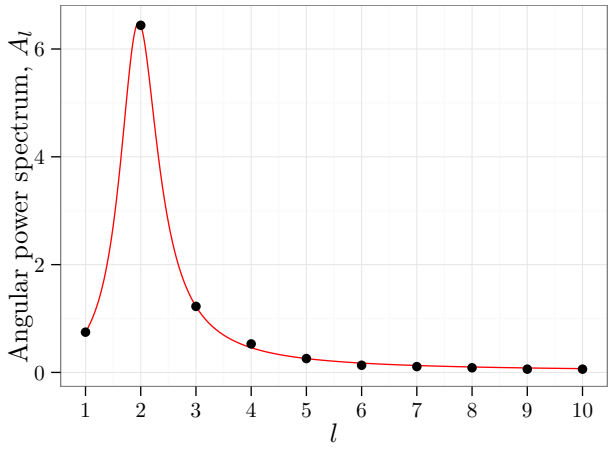

Fig. 4. Example of an angular power spectrum. Reprinted from [16] with permission from Elsevier.

It turns out that this approach works well and that the simulated particles are in good accordance with the particles from the experimental samples, even for very differently shaped particles, see [12, 16].

Host lattice, particle arrangement. As electrode materials can have high volume fractions of active materials (up to 73%, see e.g., [12]) one major challenge is to create a dense packing of irregularly shaped particles. There exist several approaches to generate dense particle structures directly from a set of particles, e.g., by using packing algorithms like the force-biased algorithm [17]. However, a huge drawback is that this approach is very time-consuming and for large observation windows it takes up to days on modern hardware. Furthermore,

dense packing algorithms are usually applied to packings of spheres. In a situation where particles are not spherical or even not convex they often cannot be applied or at least are way more complex.

Moreover, the particles (that will be generated later with the model described above) have high connectivity. Thus, an indirect approach for the placement of particles is used. First, a 'host lattice' is generated consisting of single polytopes where particles will be placed inside in the next step.

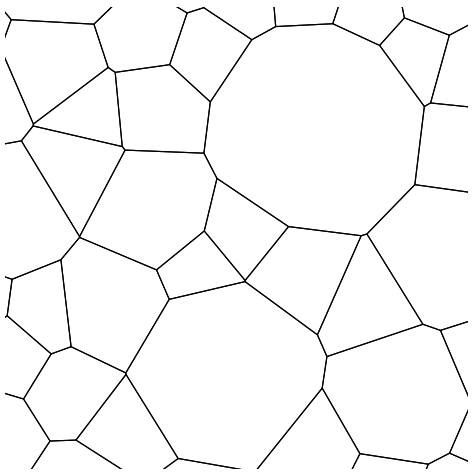

Fig. 5. 2D intersection of a Laguerre tesselation. Reprinted from [16] with permission from Elsevier.

A Laguerre tessellation is used as 'host lattice', which is a division of the space into disjoint convex polytopes. In more detail, a random tessellation [18] is used as this gives great flexibility but can also be generated efficiently as Laguerre diagram of a random marked point pattern, see Fig. 5. The generation of a 'host lattice' for particle placement has to be adopted for different materials. This means that the random point pattern for the generation of the Laguerre tessellation has to be fitted to each case, and in some applications not all polytopes are used as particle hosts but some are left empty.

Connectivity of the particles. As emphasized before, the high connectivity of particles is very important for electrode materials. Thus, this property has to be incorporated in the model. This is done by using a random graph which contains the corresponding information, the so-called connectivity graph. The nodes of this graph correspond to the polytopes of the tessellation and an edge in the graph indicates that the particles, that will be placed in two polytopes later on, have to be in contact with each other.

Two polytopes are said to be neighboring if they share a common facet. Thus, facets of the tessellation can be seen as edges of the connectivity graph. An example of such a graph is shown in Fig. 6.

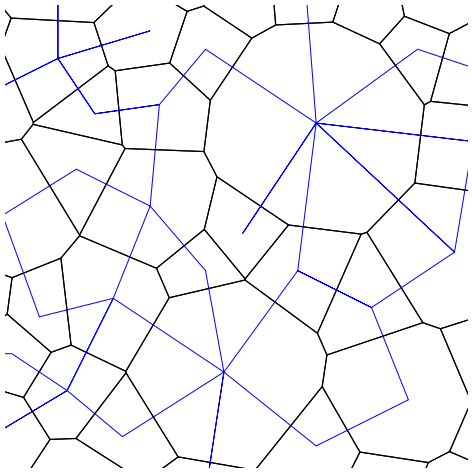

Fig. 6. Example of a connectivity graph (blue) and the underlying tessellation (black). Reprinted from [16] with permission from Elsevier.

One important side condition is, as stated above, that there are no particles or clusters of particles that have no connection to the rest of the system. This means that for each particle there has to be a path of connections to every other particle in the bulk. This can be achieved by a special construction algorithm of the graph as follows. After the generation of the tessellation, first the graph of full connectivity is generated. This means the polytopes in the observation window are taken as vertices and for the edges, every facet is turned into an edge that connects the two polytopes that share this facet. Thus, in this graph each node is connected to all its neighbors. Depending on the application a weighting of the edges can be applied.

Then, the minimum spanning tree (MST) of the graph of full connectivity is calculated. The MST is the minimal subgraph which fulfills the condition that there exists a path from every node to every other node in the graph [19].

The MST forms the basis for the connectivity graph. This final connectivity graph is then generated by adding edges between neighboring nodes based on a Bernoulli experiment, where the edge-putting probability is given by variations of the following different model types:

- The probability is fixed and independent of the polytope / particle.
- The probability is given as a function of characteristics (like the surface area) of the common facet.
- The probability depends on the angle of the connection of the centroids of the two neighboring polytopes.

– The probability depends on the distance between the centroids of the two polytopes.

The latter option is especially necessary if the electrode microstructure is anisotropic. More details can be found in [20].

Particle placement and boundary conditions. Given the model for the particle shapes based on the GRFs on the sphere, particles are placed inside polytopes of the tessellation.

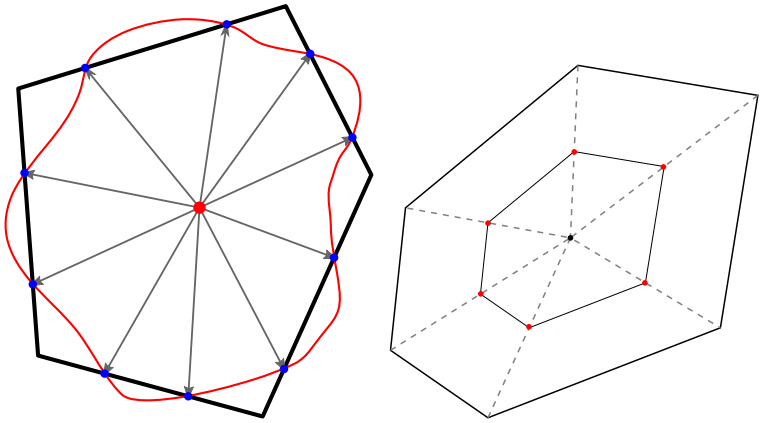

Fig. 7. (a) 2D schema of the boundary conditions. Particle (red) and surrounding polytope (black). The boundary conditions are that the particle touches the facet at specific points (blue). These conditions are also generated for the neighboring particles, thus it is ensured that both particles touch each other. (b) Boundary conditions on the facet (red dots). Both neighboring particles have to touch several points on their common facet and thus are connected. Reprinted from [16] with permission from Elsevier.

Furthermore, the following two rules are used for the particle placement:

– A particle's shape should roughly follow the shape of the polytope.
– A particle has to touch its neighbors according to the edges of the connectivity graph.

Generally, the particles should have shapes that are characteristic for the material. This is ensured by using realizations of the particle model explained above. As the particles are placed inside the Laguerre polytopes, their barycenters are used as origins of spherical coordinate systems. The particles are then represented as an expansion in spherical harmonic functions whose coefficients are generated from the GRF model described above.

Simulation of individual particles. The last step for the generation of a simulated microstructure is the generation of particles. On the one hand, they need to be generated from the (stochastic) model described above and on the other hand they need to fulfill the boundary conditions explained previously.

This is indeed possible due to the special nature of the particle model where a corresponding sampling algorithm has been developed. The basic idea is that the rules defined above can be translated into linear boundary conditions for the coefficients in the spherical harmonics expansion of the particles. As the coefficients are then sampled from a GRF model, the problem can be translated to drawing coefficients from a multivariate Gaussian distribution with boundary conditions. To make the simulation more efficient the distribution is transformed to a distribution whose realizations always fulfill the boundary conditions. Further details are given in [16].

3 Simulation of particulate materials.

Using the method for modeling and simulation of individual particles described above, it is possible to build models for different kinds of electrode materials. Electrodes in so-called energy cells like the ones used in electric vehicles have high particle densities and relatively small porosities.

The simulated 3D microstructures are then used for spatially resolved transport simulations [21] where the focus is put on the electrochemical validation of the simulated microstructures. Moreover, in [5], the electrochemical simulations performed on simulated 3D microstructures are combined with model order reduction methods to accelerate the whole procedure which enables the simulation of multiple cycles, e.g., for virtual aging tests.

In lithium-ion cells designed for power applications like the ones used in plugin hybrid vehicles, the volume fraction of active material is lower but the specific surface area is higher to allow for higher charge and discharge currents. Such 3D microstructures have been simulated with an extended version of the modeling approach described above for energy cells, where a refined tessellation model is used and some polytopes are left empty when placing the particles [20].

The counterpart of the anode in a lithium-ion battery cell is the positive electrode, also called cathode. The considered cathodes of plugin hybrid energy cells exhibit low volume fractions of active material, a different particle connectivity and especially nearly spherical particle shapes. By adaptions and enhancements of the above two modeling approaches for anodes, it is possible to use the general framework also for simulation of 3D cathode microstructures.

In the following the different applications of the general framework described above and the adaptions are discussed in more detail.

3.1 Anode of an energy cell

The main difficulty for the simulation of anodes that are optimized for a large energy density is the high volume fraction of active material. In our case the

volume fraction of active material is about 73 %. Therefore, one of the main challenges is to generate realistic structures with such a high volume fraction but still realistic particles and the high connectivity present in the material.

Host lattice, particle arrangement. The generation of the host lattice is based on a point pattern generated by a so-called random sequential adsorption process (RSA) [22, 23]. This leads to point patterns that have some 'regularity'. This means that, with a high probability, there will be no isolated points as well as no clustering of points. The 'host lattice' is then obtained by calculating the Laguerre diagram of the realization of the RSA process.

Connectivity of the particles Based on the minimum spanning tree of the graph of full connectivity, edges are added with a probability proportional to the area of the facet between two neighboring polytopes. Fig. 7 shows the boundary conditions that are applied to the particles in detail.

Simulation of individual particles. The particles are simulated using the GRF model described above with an angular power spectrum that has been fitted to the particles extracted from tomographic images. The angular power spectrum is shown in Fig. 4. A comparison of the experimental structure and the result of model-based simulation is shown in Fig. 1.

3.2 Anode of a power cell

The microstructure of power cell anodes strongly differs from the one in energy cell anodes. While both consist of a completely connected system of particles (the so-called active material), the volume fraction of the active material is much lower for power cell anodes. This improves transport properties in the pore phase. Thus, the stochastic microstructure model for energy cell anodes has to be adapted to capture this property. Besides some smaller modifications, which include a dependence of the connectivity graph on the spatial orientation of pairs of particles to each other in order to include the anisotropy that was observed in tomographic image data, the main difference is the inclusion of empty polytopes in the host lattice, where no particles are created in. This allows to account for the low volume fraction of the active material, while preserving realistic shapes of particles.

Host lattice, particle arrangement. The generation of the host lattice is again based on a system of spheres, which is simulated using a modification of the so-called force-biased algorithm [24]. Based on an initial configuration of spheres, an iterative rearrangement is performed until the overlap of spheres falls below a certain threshold. This procedure results in a system of spheres which resembles the properties of the particle system observed in tomographic image data, represented as spheres with volume-equivalent radii. Based on this, the corresponding Laguerre tessellation can be computed, which results in a space-filling system of polytopes.

Connectivity of the particles. Given the Laguerre tessellation, a graph indicating connectivity between particles is created. To account for the anisotropic shape of particles observed in tomographic image data, the graph is created such that particles are rather connected in horizontal direction than in vertical direction. This means that, besides the size of the Laguerre facet between two points and the distance of those points, the angle with respect to horizontal direction between those points is computed. Starting with a minimum spanning tree to ensure complete connectivity, edges are added based on those three characteristics with a probability such that the mean coordination number of the graph extracted from tomographic image data is matched.

Modification of host lattice to include empty polytopes. Particles need to fulfill the connectivity conditions induced by the graph on the one hand, but on the other hand they have to preserve the desired size. This is important to match the volume fraction of active material in the electrode. Therefore, the polytopes where particles are placed in are made smaller by including empty polytopes into the space-filling system. These empty polytopes are found by adding points to the generators of the Laguerre tessellation at the center of those facets where no connectivity is induced by the graph. Moreover, it is ensured that the resulting empty polytopes do not remove facets of the tessellation where two particles are supposed to be connected.

Simulation of individual particles. Finally, the particles are modeled using spherical harmonics in the polytopes that have been made smaller in the preceding step. Because of the smaller polytopes, most particles can fulfill their connectivity conditions and required size together with a reasonable shape. In case this is problematic, a more flexible way of setting the boundary conditions to account for the connectivity is used. For details, we refer to [20]. A comparison of a model output to tomographic image data can be found in Fig. 8.

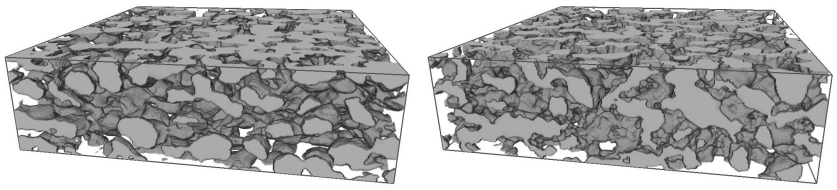

(a) (b)

Fig. 8. Comparison of cutout of tomographic image data for a power cell anode (a) and corresponding model realization (b).

3.3 Cathode of an energy cell

After having applied the general framework to model and simulate the 3D microstructure of two kinds of anodes, namely the ones in lithium-ion energy and power cells, a third application of the framework concerns modeling and simulation of cathode microstructures (pristine as well as cyclically aged structures). Cathode microstructures also exhibit distinct structural characteristics which made some adaptations necessary. There are three main structural differences observed in cathodes.

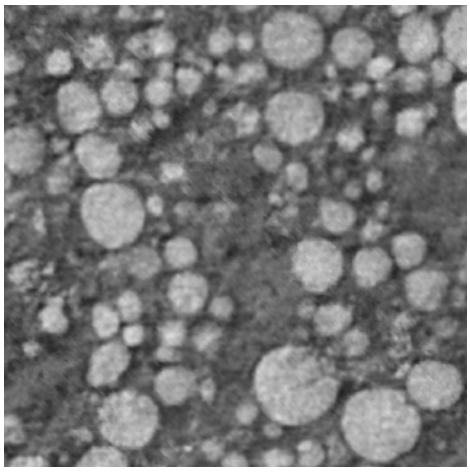

Fig. 9. Tomographic grayscale image - 2D slice of a cutout - showing the microstructure of a pristine cathode.

Host lattice, particle arrangement. First, there are locally occurring large pores, especially in the case of the pristine cathode. Therefore, when arranging the placement of particles in a similar way as done for power cell anodes, a random marked point pattern is simulated which explicitly generates large polytopes in the host lattice into which no particles are placed later on. These large and empty polytopes mimic large pores in the simulated microstructure.

Connectivity of particles. Further, cathodes for lithium-ion batteries exhibit another particle connectivity than anodes. That means, the particle system forming the cathode microstructure is not necessarily fully connected anymore as observed in the anode cases. This characteristic feature is captured by omitting the previously used tool of a minimum spanning tree when creating the connectivity graph. Instead, the probability that a pair of particles is connected depends on just two criteria which are determined from the host lattice, see [25] for details. The result is a suitable particle connectivity graph.

Particle placement, boundary conditions and simulation of individual particles. The third and most obvious microstructural difference are the nearly spherical-shaped particles in the cathodes, see Fig. 9. To achieve simulated particles of such shapes, we proceed in three steps:

- The polytopes in the host lattice into which particles will be placed are shrunken to nearly spherical shapes by adding further polytopes which remain empty.
- The number of boundary (contact) conditions per particle is reduced, i.e., now there is only one boundary condition (point) per facet, compare Fig. 7, which guarantees connectivity as claimed by the graph.
- The parameter L at which the series of spherical harmonic functions is truncated is no longer fixed for each particle but dynamically chosen depending on the number of connected neighboring particles. This number is also called the coordination number of a particle and it is known for each particle from the connectivity graph. At the end, a higher number of connected neighboring particles means a larger L and, vice versa, a smaller coordination number means a smaller L.

All three steps lead to less restricted and less degenerated particles and allow them to have nearly spherical shapes as desired.

To give a short overview, the basic ideas of the application of the general framework to cathodes of an energy cell are summarized and illustrated by 2D sketches in Fig. 10.

3.4 Applications of simulated structures

The main fields of application for microstructure models of energy materials is the design of new structures with better functionality due to structural improvements. This is done with a method which we call virtual materials testing. The idea is to generate virtual structures from the models where the parameters are varied in a certain range around the values determined for real materials. This gives us microstructures that are realistic in the sense that they can be manufactured with known production processes on the one hand. On the other hand, these microstructures differ from the known ones and can possibly have more preferable properties. A similar procedure is used in [9, 26] to investigate the relation between microstructure and charge transport properties.

As the models introduced above reconstruct microstructures of lithium-ion cell electrodes, the functionality or performance of the material has to be determined by spatially resolved electrochemical simulations. The theoretical background is described in [3, 4].

For anodes of energy cells the microstructure model has been validated using the electrochemical simulation model [21] where it has been shown that there is a good agreement of the functional performance of virtual and experimental microstructures, see Fig. 11.

Furthermore, a workflow was developed to automatize the whole process and also to speed up the simulation of many cycles which is necessary for studies on the aging of the cells. This workflow is described in detail in [5].

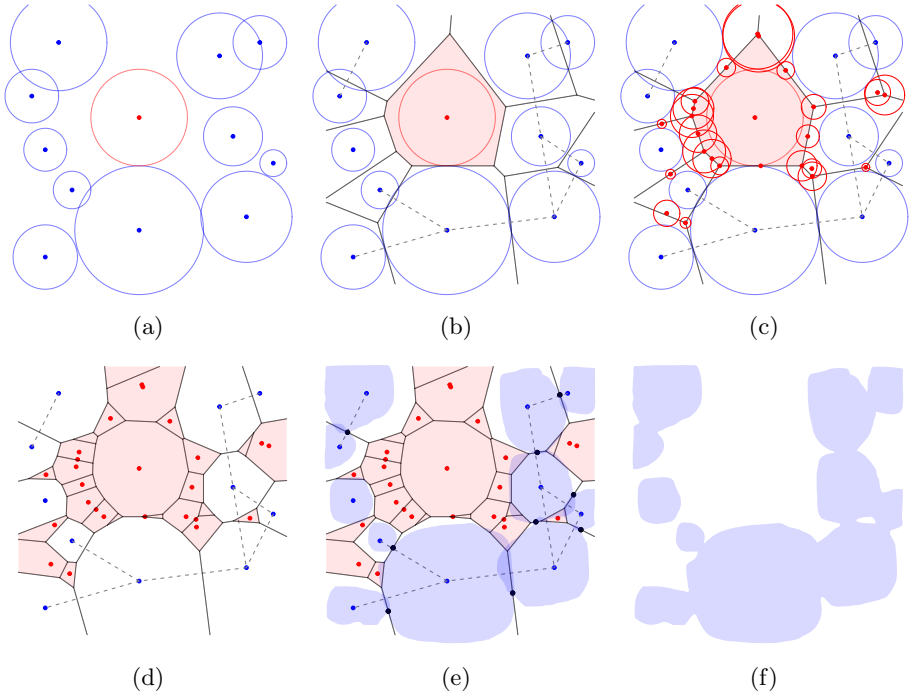

Fig. 10. Overview of the basic cathode modeling ideas. (a) Two random marked point patterns are realized, where the blue dots and circles induce particles and the red ones induce large pores; (b) A connectivity graph (dashed gray lines) based on the random marked point patterns and the corresponding Laguerre tessellation (black lines) is simulated, where the red shaded polytope indicates an (empty) pore polytope (i.e., no particle is placed into); (c) Additional marked points (further red dots and circles) are determined that induce further pore polytopes; (d) Final arrangement of particle polytopes (i.e., a particle is placed into) and pore polytopes (red shaded) is computed, where the initial connectivity is still retained; (e) Particles fulfilling boundary conditions (black dots) are created in the corresponding polytopes using spherical harmonics; (f) Only the particles are kept and morphological smoothing operations lead to the final particle system.

4 Summary, related work & outlook

A general framework for the simulation of battery electrode microstructures is presented. The framework consists of multiple steps that can be adopted for a wide range of electrode materials. Three microstructure models for different electrodes of lithium-ion cells based on this framework are considered. Finally, a validation of the model using spatially resolved electrochemical simulations is mentioned and further applications of such microstructure models are discussed.

Currently, the modeling tools are extended to incorporate cracked particles. In [27], an application of machine learning for the detection of broken particles

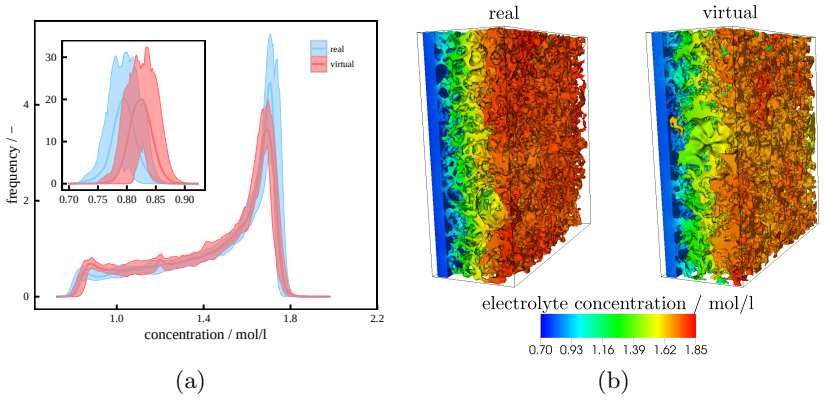

(a) (b)

Fig. 11. (a) The distribution of the electrolyte concentration for the electrode pore space and the separator (inset). The density is normed to unity area. The small peak at the initial concentration indicates unconnected pore volume. (b) Spatial distribution of electrolyte concentration for two cut-outs: real (left) and virtual (right). Both have the same color scale (shown below). Larger particles can be seen in both structures. Also both cut-outs show electrolyte pores, which are less connected to the main pore space: (virtual) orange part close to the blue and (real) dark red at the upper corner. Reprinted from [21] with permission from Elsevier.

in tomographic images for negative electrode materials of lithium-ion batteries has been proposed. In [28], an approach for structural segmentation of defective particles has been developed, which also accounts for cracks and holes in particles. The automated detection of cracked particles combined with the parametric representation of individual particles described above enables statistical investigations of the relationship between the morphology of particles and their cracking behavior.

Furthermore, investigations of the influence of different degrees of compression or multi-layered constructions of positive electrode materials on the properties of lithium-ion batteries, e.g., on their ion transport behavior, are possible using the tools described in the present paper.

References

1. Remmlinger, J., Tippmann, S., Buchholz, M., Dietmayer, K.: Low-temperature charging of lithium-ion cells Part II: Model reduction and application. Journal of Power Sources **254** (2014) 268–276
2. Newman, J., Thomas, K., Hafezi, H., Wheeler, D.: Modeling of lithium-ion batteries. Journal of Power Sources **119** (2003) 838–843
3. Latz, A., Zausch, J.: Thermodynamic consistent transport theory of Li-ion batteries. Journal of Power Sources **196** (2011) 3296–3302
4. Latz, A., Zausch, J.: Thermodynamic derivation of a Butler-Volmer model for intercalation in Li-ion batteries. Electrochimica Acta **110** (2013) 358–362

5. Feinauer, J., Hein, S., Rave, S., Schmidt, S., Westhoff, D., Zausch, J., Iliev, O., Latz, A., Ohlberger, M., Schmidt, V.: MULTIBAT: Unified workflow for fast electrochemical 3D simulations of lithium-ion cells combining virtual stochastic microstructures, electrochemical degradation models and model order reduction. arXiv:1704.04139 (2017)
6. Gaiselmann, G., Neumann, M., Holzer, L., Hocker, T., Prestat, M., Schmidt, V.: Stochastic 3D modeling of LSC cathodes based on structural segmentation of FIB-SEM images. Computational Materials Science **67** (2013) 48–62
7. Gaiselmann, G., Thiedmann, R., Manke, I., Lehnert, W., Schmidt, V.: Stochastic 3D modeling of fiber-based materials. Computational Materials Science **59** (2012) 75–86
8. Stenzel, O., Koster, L., Thiedmann, R., Oosterhout, S., Janssen, R., Schmidt, V.: A new approach to model-based simulation of disordered polymer blend solar cells. Advanced Functional Materials **22** (2012) 1236–1244
9. Stenzel, O., Pecho, O., Holzer, L., Neumann, M., Schmidt, V.: Predicting effective conductivities based on geometric microstructure characteristics. AIChE Journal **62**(5) (2016) 1834–1843
10. Münch, B., Holzer, L.: Contradicting geometrical concepts in pore size analysis attained with electron microscopy and mercury intrusion. Journal of the American Ceramic Society **91**(12) (2008) 4059–4067
11. Pfaffmann, L., Birkenmaier, C., Müller, M., Bauer, W., Mitsch, T., Feinauer, J., Scheiba, F., Hintennach, A., Schleid, T., Schmidt, V., Ehrenberg, H.: Investigation of the electrochemical active surface area and lithium diffusion in graphite anodes by a novel OsO4 staining method. Journal of Power Sources **307** (2016) 762–771
12. Feinauer, J., Spettl, A., Manke, I., Strege, S., Kwade, A., Pott, A., Schmidt, V.: Structural characterization of particle systems using spherical harmonics. Materials Characterization **106** (2015) 123–133
13. Gaiselmann, G., Neumann, M., Holzer, L., Hocker, T., Prestat, M.R., Schmidt, V.: Stochastic 3d modeling of $La_{0.6}Sr_{0.4}CoO_{3-\delta}$ cathodes based on structural segmentation of FIB–SEM images. Computational Materials Science **67** (2013) 48–62
14. Chen, C.F., Mukherjee, P.P.: Probing the morphological influence on solid electrolyte interphase and impedance response in intercalation electrodes. Physical Chemistry Chemical Physics **17**(15) (2015) 9812–9827
15. Cho, S., Chen, C.F., Mukherjee, P.P.: Influence of microstructure on impedance response in intercalation electrodes. Journal of the Electrochemical Society **162**(7) (2015) A1202–A1214
16. Feinauer, J., Brereton, T., Spettl, A., Weber, M., Manke, I., Schmidt, V.: Stochastic 3D modeling of the microstructure of lithium-ion battery anodes via Gaussian random fields on the sphere. Computational Materials Science **109** (2015) 137–146
17. Mościński, J., Bargieł, M., Rycerz, Z., Jacobs, P.: The force-biased algorithm for the irregular close packing of equal hard spheres. Molecular Simulation **3**(4) (1989) 201–212
18. Lautensack, C., Zuyev, S.: Random Laguerre tessellations. Advances in applied probability **40**(3) (2008) 630–650
19. Graham, R.L., Hell, P.: On the history of the minimum spanning tree problem. Annals of the History of Computing **7**(1) (1985) 43–57
20. Westhoff, D., Feinauer, J., Kuchler, K., Mitsch, T., Manke, I., Hein, S., Latz, A., Schmidt, V.: Parametric stochastic 3D model for the microstructure of anodes in lithium-ion power cells. Computational Materials Science **126** (2017) 453–467

21. Hein, S., Feinauer, J., Westhoff, D., Manke, I., Schmidt, V., Latz, A.: Stochastic microstructure modeling and electrochemical simulation of lithium-ion cell anodes in 3D. Journal of Power Sources **336** (2016) 161–171
22. Chiu, S.N., Stoyan, D., Kendall, W.S., Mecke, J.: Stochastic Geometry and its Applications. 3rd edition edn. J. Wiley & Sons (2013)
23. Torquato, S.: Random Heterogeneous Materials: Microstructure and Macroscopic Properties. Springer (2002)
24. Bezrukov, A., Bargie, M., Stoyan, D.: Statistical analysis of simulated random packings of spheres. Particle & Particle Systems Characterization **19**(2) (2002) 111–118
25. Kuchler, K., Westhoff, D., Feinauer, J., Mitsch, T., Manke, I., Schmidt, V.: Stochastic model of the 3D microstructure of Li-ion battery cathodes under various cyclical aging secenarios. arXiv:1710.02051 (2017)
26. Gaiselmann, G., Neumann, M., Schmidt, V., Pecho, O., Hocker, T., Holzer, L.: Quantitative relationships between microstructure and effective transport properties based on virtual materials testing. AIChE Journal **60**(6) (2014) 1983–1999
27. Petrich, L., Westhoff, D., Feinauer, J., Finegan, D.P., Daemi, S.R., Shearing, P.R., Schmidt, V.: Crack detection in lithium-ion cells using machine learning. Computational Materials Science **136** (2017) 297–305
28. Westhoff, D., Finegan, D.P., Shearing, P.R., Schmidt, V.: Algorithmic structural segmentation of defective particle systems: A lithium-ion battery study. Journal of Microscopy (in print, doi: 10.1111/jmi.12653)